Performance of a CDMA Beamforming Array-Receiver in Spatially-Correlated Rayleigh-Fading Multipath*

Sofiène AFFES and Paul MERMELSTEIN
INRS-Télécommunications, Université du Québec
16, Place du Commerce, Ile-des-Soeurs, Verdun, H3E 1H6, Canada

Abstract—**In previous work we proposed an array-receiver that implements coherent maximum ratio combining (MRC) in space and time in a 2D-RAKE structure. In this contribution we evaluate different versions of this combiner in spatially-correlated Rayleigh fading and compare them to previous array-receiver solutions. Simulation results indicate that the proposed versions are more sensitive to spatial correlation, especially those which better exploit spatial combining. However, they still offer the best performance even in very poor spatial diversity situations. Results also suggest that concatenated processing of the spatio-temporal components significantly increases robustness to correlation and further improves the performance advantage over 2D-RAKE structures.**

I. Introduction

Adaptive antenna-beamforming achieves a significant capacity increase in multiple access spread spectrum techniques. Standards proposals for the third-generation personal communication systems based on CDMA [1] plan to integrate smart antennas on both links. Antenna processing benefits include improved exploitation of spatial diversity and rejection or reduction (*i.e.*, antenna gain) of interference. Antenna sectorization of IS-95 CDMA [2] can be replaced by square law combining over antennas [3] to exploit spatial diversity efficiently. Array-beamforming over antennas, implemented in a 2D-RAKE structure [4] further exploits the interference reduction achievable with multiple antennas. Additional improvements lead to better exploitation of the antenna processing capabilities by coherent detection without a pilot [5],[6].

However, one major concern with antenna arrays is the antenna spacing at the base and/or the mobile-stations, which may limit the benefits derived from use of multiple antennas. To minimize size and weight, antenna spacing should be kept to a minimum. As the antenna elements get closer, the spatial correlation between the paths to different antennas increases, thereby reducing the spatial diversity gain of the antenna array. Previous experimental studies [7],[8] assessed the effect of correlation of Rayleigh fading between two antennas on the performance of a simple diversity combining scheme and revealed that spatial diversity cannot be exploited properly beyond a critical crosscorrelation threshold of 0.7.

In addition to spatial diversity, array-receivers also achieve efficient interference reduction by antenna beamforming. In this contribution, we evaluate the effects of spatial correlation on versions of the subspace-tracking array-receiver (STAR), the CDMA beamforming array-receiver previously studied [5] for the uplink of the IS-95 [2] in an independent Rayleigh fading environment. Evaluation results indicate that the degradation in performance of array-receivers becomes noticeable only at very high values of the correlation factor between antennas, thereby confirming that antenna arrays achieve significant interference reduction even when the spatial diversity gains are significantly reduced. They also suggest that array-receivers which implement efficient array processing and exploit spatial combining better are more sensitive to spatial correlation, especially in nonselective fading. Their degradation in performance is more abrupt. However, they still offer the best performance even at very high values of the correlation factor.

* This work was supported by the Bell Quebec/Nortel/NSERC Industrial Research Chair in Personal Communications.

II. Assumptions and Overview

We briefly describe the data model and state the assumptions that are relevant to the understanding of this contribution. We also give a short overview of the tested array-receivers. More details can be found in [5].

A. Signal Model

We denote by M the number of receiving antenna elements at the base-station, by P the number of resolvable multipaths in a Rayleigh fading environment, and by L the number of Walsh correlators in IS-95 CDMA. The $(M \times 1)$-dimensional postcorrelation vector of the i-th Walsh correlator for the p-th path is therefore given by:

$$Z^i_{p,n} = G_{p,n}\psi_n\varepsilon_{p,n}\delta^i_n + N^i_{p,n} = G_{p,n}s^i_{p,n} + N^i_{p,n} \ , \qquad (1)$$

where ψ^2_n is the total received power and $\varepsilon^2_{p,n}$ for $p = 1, \ldots, P$ are the normalized power fractions over the P multipaths (*i.e.*, $\sum_{p=1}^{P} \varepsilon^2_{p,n} = 1$). $G_{p,n}$ is the $(M \times 1)$-dimensional propagation vector over the p-th path, whose norm is fixed for convenience to $\sqrt{M}$ [5]. For each multipath-delay, we assume that the corresponding M diversity paths received at the different antennas are spatially correlated, in contrast to [5] where the paths were assumed uncorrelated. It is reasonable to retain the assumption that the additive noise vector $N^i_{p,n}$ is a spatially and temporally uncorrelated Gaussian noise independent for each path and for each antenna. In the presence of a large number of users, this assumption still holds even in the presence of spatial correlation when the complex correlation factor between each couple of antennas has a different phase from one mobile to another. Otherwise, we may incorporate the near-far resistant solution in [9] for colored noise situations (*e.g.*, on the downlink), but that is beyond the scope of this

paper. Finally, δ_n^i is the binary result at iteration n of correlating the received Walsh symbol, say $w_n \in \{1,\ldots,L\}$, by the i-th Walsh correlator and $s_{p,n}^i = \psi_n \varepsilon_{p,n} \delta_n^i$ is the corresponding signal component.

The postcorrelation model over each path of Eq. (1) is appropriate for processing of array signal vectors over multipath fingers in a 2D-RAKE [4] structure (*i.e.*, sequential combining over antennas and over multipaths). For explicit spatio-temporal processing, we introduce the postcorrelation model (PCM) developed in [6]. Assuming perfect synchronization of multipath delays in terms of multiples of the chip duration, we can restrict the postcorrelation matrix in [6] at the output of the i-th Walsh correlator to the $M \times P$ diversity branches available as follows:

$$\mathbf{Z}_n^i = \left[Z_{1,n}^i, \ldots, Z_{P,n}^i\right]. \tag{2}$$

Similarly, we form the matrices $\mathbf{G}_n$ and $\mathbf{N}_n^i$. We obtain the spatio-temporal postcorrelation observation vector of the i-th Walsh correlator by reshaping $\mathbf{Z}_n^i$ as:

$$\underline{Z}_n^i = \underline{G}_n \psi_n \delta_n^i + \underline{N}_n^i = \underline{G}_n s_n^i + \underline{N}_n^i \,, \tag{3}$$

where $s_n^i = \psi_n \delta_n^i$ is the spatio-temporal signal component. The spatio-temporal propagation and noise vectors $\underline{G}_n$ and $\underline{N}_n^i$ result from the transformation of $\mathbf{G}_n$ diag $([\varepsilon_{1,n}, \ldots, \varepsilon_{P,n}])$ and $\mathbf{N}_n^i$, respectively. We show next that concatenated spatio-temporal combining exploiting the PCM model outperforms 2D-RAKE processing.

B. The Tested Array-Receivers

In Tab. 1, we provide the decision variables of the tested array-receivers. Those of Tab. 1a, 1b, 1c and 1e were previously studied in [5]. Those of Tab. 1d and 1f are new versions. We briefly describe their structure below.

The first scheme is diversity combining. It achieves noncoherent reception by spatio-temporal square law combining (ST-SLC) of the postcorrelation data over the $M \times P$ diversity branches [3]. We refer to this scheme as ST-SLC and S-SLC in selective and nonselective fading, respectively (see Tab. 1a).

If a channel estimate is available within a phase ambiguity, *i.e.*, $\hat{G}_{p,n} \simeq e^{-j\phi_{p,n}} G_{p,n}$, antenna beamforming can be applied to achieve differential spatial maximum ratio combining (D.S-MRC) of the postcorrelation data over each multipath. Due to the unknown angular rotations over the paths, the beamformer outputs are fed to a temporal square law combiner (T-SLC or E for energy in nonselective fading) to achieve noncoherent combining [4] with improved performance over diversity combining. We refer to this scheme as D.S-MRC/T-SLC and D.S-MRC/E in selective and nonselective fading, respectively (see Tab. 1b).

In [5], we proposed signal processing improvements to this antenna beamforming scheme and proposed the subspace-tracking array-receiver (STAR). With the aid of decision feedback identification (DFI), we first achieved a 3 dB coherent detection gain in interference reduction without a pilot by spatial MRC (S-MRC). We refer to this modified scheme as S-MRC/T-SLC and S-MRC/E in selective and nonselective fading, respectively (see Tab. 1c). We then replaced temporal SLC by temporal MRC (T-MRC) to achieve an additional enhancement of the receiver performance. We refer to the resulting scheme as S-MRC/T-MRC and S-MRC in selective and nonselective fading, respectively (see Tab. 1e).

The simulations will indicate that the decision variables which exploit diversity better are more sensitive to greater spatial correlation. To increase the robustness of S-MRC/T-MRC, we test a new decision variable (see Tab. 1d) corresponding to the square of the decision variable previously used (see Tab. 1e). We refer to this scheme as S-MRC/T-MRC/E and S-MRC/E in selective and nonselective fading, respectively (see Tab. 1d).

The above decision variables rely on channel estimation (except for ST-SLC). STAR is able to feed back signal component estimates from any of these decisions to achieve channel identification in a simple DFI scheme [5] by:

$$\hat{G}_{p,n+1} = \hat{G}_{p,n} + \mu_{p,n} \left(Z_{p,n}^{\hat{w}_n} - \hat{G}_{p,n} \widehat{s_{p,n}^{w_n}}\right) \widehat{s_{p,n}^{w_n}} \,, \tag{4}$$

where $\mu_{p,n}$ is an adaptation step-size and $\widehat{s_{p,n}^{w_n}}$ is the signal component estimate (not to be confused with $\hat{s}_{p,n}^{\hat{w}_n}$) obtained after hard decision (*i.e.*, $\hat{w}_n$) and received power estimation (*i.e.*, $\hat{\psi}_n^2$ and $\hat{\varepsilon}_{p,n}^2$) [5]. We can always feed back $\widehat{s_{p,n}^{w_n}} = \hat{\varepsilon}_{p,n} \hat{\psi}_n$ in Eq. (4) to achieve channel identification without ambiguity (*i.e.*, $\phi_{p,n} = 0$). For illustration purposes, we provide in Tab. 1 different feedback signals that better justify the choice of the corresponding decision variables from the resulting ambiguities.

From the PCM model of Eq. (3) we can derive another decision variable which concatenates the 2D-RAKE structure of S-MRC/T-MRC along a single spatio-temporal (ST) dimension. We refer to this scheme as ST-MRC and S-MRC in selective and nonselective fading, respectively (see Tab. 1f). Channel identification of Eq. (4) is replaced in this scheme by:

$$\hat{\underline{G}}_{n+1} = \hat{\underline{G}}_n + \mu_n \left(\underline{Z}_n^{\hat{w}_n} - \hat{\underline{G}}_n \widehat{s_n^{w_n}}\right) \widehat{s_n^{w_n}} \,, \tag{5}$$

where μ_n is an adaptation step-size and $\widehat{s_n^{w_n}} = \hat{\psi}_n$ is the spatio-temporal signal component estimate. STAR with ST-MRC does not require the estimation of the power fractions and hence reduces identification errors. We shall see in the next section that it outperforms previous array-receiver solutions.

III. Evaluation Results

We evaluate the uplink performance of the array-receivers described in the previous section in terms of the bit error rate (BER), the required signal-to-noise ratio (SNR) at a BER of 10^{-3} and the resulting capacity, C, in number of users per cell. We assess their degradation as a function of the spatial correlation of Rayleigh fading between the two receiving antennas at the base-station (*i.e.*, $M = 2$).

	decision rule	feedback signal	ambiguity
(a)	$d_n^i = \frac{\|\underline{Z}_n^i\|^2}{M}$	none	no id.
(b)	$\hat{s}_{p,n}^i = \frac{\hat{G}_{p,n}^H Z_{p,n}^i}{M} \longrightarrow d_n^i = \sum_{p=1}^{P} \|\hat{s}_{p,n}^i\|^2$	$\widehat{s_{p,n}^{w_n}} = \hat{s}_{p,n}^{\hat{w}_n}$	$\phi_{p,n} \in [0, 2\pi]$
(c)	$\hat{s}_{p,n}^i = \mathrm{Re}\left\{\frac{\hat{G}_{p,n}^H Z_{p,n}^i}{M}\right\} \longrightarrow d_n^i = \sum_{p=1}^{P} \|\hat{s}_{p,n}^i\|^2$	$\widehat{s_{p,n}^{w_n}} = \hat{s}_{p,n}^{\hat{w}_n}$	$\phi_{p,n} \in \{0, \pi\}$
(d)	$\hat{s}_{p,n}^i = \mathrm{Re}\left\{\frac{\hat{G}_{p,n}^H Z_{p,n}^i}{M}\right\} \longrightarrow \hat{s}_n^i = \sum_{p=1}^{P} \hat{\varepsilon}_{p,n} \hat{s}_{p,n}^i \longrightarrow d_n^i = \|\hat{s}_n^i\|^2$	$\widehat{s_{p,n}^{w_n}} = \hat{\varepsilon}_{p,n} \hat{\psi}_n \ \mathrm{Sign}\{\hat{s}_n^i\}$	all $\phi_{p,n} = \begin{cases} 0 \\ \pi \end{cases}$
(e)	$\hat{s}_{p,n}^i = \mathrm{Re}\left\{\frac{\hat{G}_{p,n}^H Z_{p,n}^i}{M}\right\} \longrightarrow d_n^i = \sum_{p=1}^{P} \hat{\varepsilon}_{p,n} \hat{s}_{p,n}^i$	$\widehat{s_{p,n}^{w_n}} = \hat{\varepsilon}_{p,n} \hat{\psi}_n$	all $\phi_{p,n} = 0$
(f)	$d_n^i = \mathrm{Re}\left\{\frac{\hat{\underline{G}}_n^H \underline{Z}_n^i}{M}\right\}$	$\widehat{s_n^{w_n}} = \hat{\psi}_n$	$\phi_n = 0$

Tab. 1. Array-receivers in nonselective fading (*i.e.*, $P = 1$) - (a): S-SLC , (b): D.S-MRC/E, (c-d): S-MRC/E, (e-f): S-MRC. Array-receivers in selective fading (*i.e.*, $P > 1$) - (a): ST-SLC, (b): D.S-MRC/T-SLC, (c): S-MRC/T-SLC, (d): S-MRC/T-MRC/E, (e): S-MRC/T-MRC, (f): ST-MRC.

A. Simulation Setup

Multipath vector channel simulators such as [10] take into account propagation conditions (*i.e.*, angular spread, array geometry, locations, etc...) to model the spatial correlation between antennas. Here, for convenience, we arbitrarily control the correlation factor, ρ, of the Rayleigh fading between the two receiving antennas and force it to be real positive and identical over all resolvable paths. Thus, we have for $p = 1, \ldots, P$:

$$E\left[\psi_n^2 \varepsilon_{p,n}^2 G_{p,n} G_{p,n}^H\right] = \bar{\varepsilon}_p^2 \begin{bmatrix} 1 & \rho \\ \rho & 1 \end{bmatrix}, \qquad (6)$$

where $\bar{\varepsilon}_p^2$ is the average power fraction. This permits the evaluation of the dependence of the above performance measures on a single spatial correlation parameter, the correlation factor ρ. We shall sample values of ρ between 0 and 1 to cover the entire range of the envelopes' crosscorrelation.

We simulate two systems having bandwidths of 1.25 and 5 MHz operating at a carrier frequency of 1.9 GHz in nonselective and selective fading environments with one (*i.e.*, $P = 1$) and three equal power paths (*i.e.*, $P = 3$), respectively. Voice users transmit at an information rate of 9.6 kbps, spread with processing gains of 128 and 512, respectively. These users are moving at a maximum speed of 1 km/h and give rise to a slow Rayleigh fading channel, generated by Jakes' model [11] with a Doppler frequency $f_D \simeq 2$ Hz. Their voice data is coded by a convolutional encoder at the rate 1/3 and mapped into 64-ary Walsh symbols at the rate of 4.8 kbaud before interleaving with a 32×6 matrix. We also update power control every 1.25 ms (*i.e.*, duration of 6 symbols) to instruct to the mobile to either increase or decrease its power by a constant step-size of 0.5 dB. This binary power control transmission experiences 10% BER and a delay of 1.25 ms. Finally, in Eqs. (4) and (5) we use a step-size μ of 0.05 for channel identification with all the studied array-receivers (except for ST-SLC).

B. BER Results

In Figs. 1 and 2, we provide performance results in terms of BER versus the input SNR per information bit[1] for different values of ρ in the nonselective and selective fading environments, respectively. The curves indicate the following:

- For all methods, the degradation in performance becomes noticeable only at very high values of the correlation factor, whether the Rayleigh fading is selective or not. This confirms that antenna arrays can still achieve efficient interference reduction despite a significant loss of spatial diversity[2].
- The array-receivers that implement efficient array processing and exploit spatial combining better are more sensitive to spatial correlation, as one would expect, except for ST-MRC. Notice that the loss in SNR becomes more significant and abrupt with higher values of ρ from Fig. 1a to Fig. 1d and from Fig. 2a to Fig. 2e. On the other hand, the SNR curves of ST-MRC in Fig. 2f remain almost constant. They suggest that

[1] In [5], we did not include in the SNR term the loss/gain in signal power due to an imperfect power control. Hence the "BER versus SNR" curves are different from those of Figs. 1 and 2 for $\rho = 0$.

[2] We verified by simulations that a receiver with $M = 2$ antennas and $\rho = 1$ performs better than with $M = 1$ antenna, although both situations offer the same spatial diversity.

the loss in performance of the most efficient 2D-RAKE based structures is due to increasing estimation errors of the power fractions (and therefore of power control).

- In nonselective fading, the degradation in performance due to spatial correlation is more pronounced. STAR with S-MRC should be used up to a correlation factor around 0.8[3]. For higher values of ρ, STAR with S-MRC/E is preferred.
- In selective fading, temporal diversity reduces the sensitivity of the array-receivers to spatial correlation. Among the 2D-RAKE based structures, STAR with S-MRC/T-MRC should be used up to a correlation factor around 0.9. For higher values of ρ, S-MRC/T-MRC/E and S-MRC/T-SLC are preferred. Correlation thresholds lie approximately at 0.9 and 0.95, respectively. However, concatenated spatio-temporal processing with ST-MRC always outperforms the best of these schemes for any tested value of ρ.

Overall, STAR with the proposed enhancements still offers the best performance for the tested values of the correlation factor ρ. In the following, we translate these improvements to required SNR and capacity for a maximum BER of 10^{-3}.

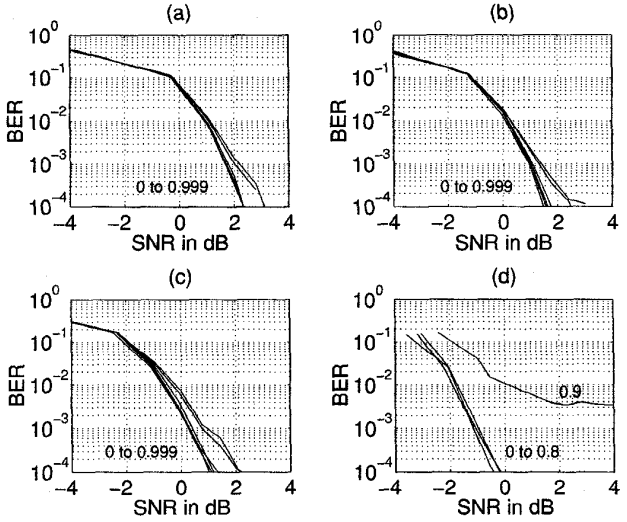

Fig. 1. BER vs. actual SNR per information bit in nonselective fading (*i.e.*, $P = 1$) for different values of ρ (0, 0.7, 0.8, 0.9, 0.99, 0.999). (a): S-SLC. (b): D.S-MRC/E. (c): S-MRC/E. (d): S-MRC.

C. Required SNR and Capacity Results

In Fig. 3, we show the required SNR performance results of the tested array-receivers for different values of ρ in the nonselective[4] and selective fading environments. Fig. 3a indicates constant SNR gains of S-MRC over ST-SLC [3] and D.S-MRC/E [4] in nonselective fading of about 2.8 and 2 dB, respectively, up to a correlation factor around 0.8. Both SNR gains degrade with S-MRC/E by about

[3]This value is close to the critical crosscorrelation threshold of 0.7 in [7],[8] beyond which spatial diversity cannot be exploited efficiently.

[4]In Fig. 3a, S-MRC cannot achieve the target BER of 10^{-3} for the last two values of ρ.

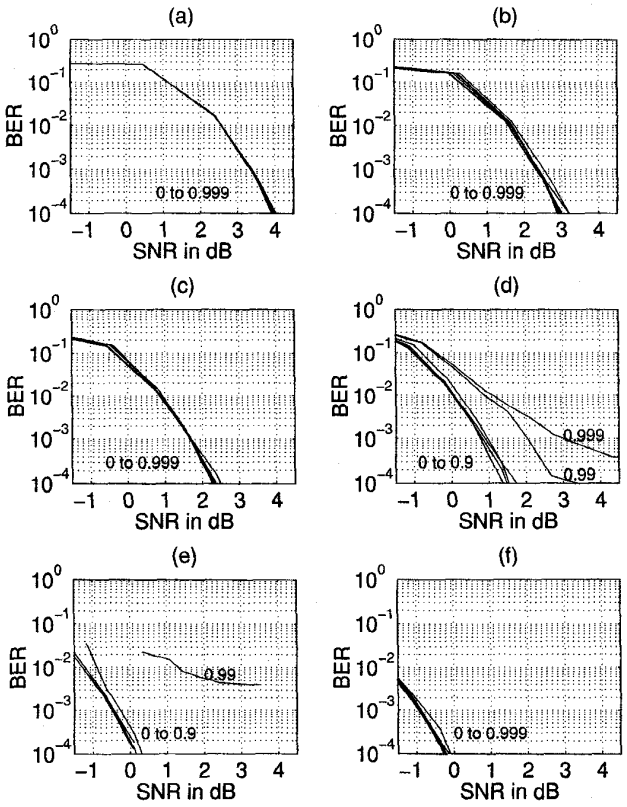

Fig. 2. BER vs. actual SNR per information bit in selective fading (*i.e.*, $P = 3$) for different values of ρ (0, 0.7, 0.8, 0.9, 0.99, 0.999). (a): ST-SLC. (b): D.S-MRC/T-SLC. (c): S-MRC/T-SLC. (d): S-MRC/T-MRC/E. (e): S-MRC/T-MRC. (f): ST-MRC.

1.4 dB at full correlation. On the other hand, Fig. 3b indicates almost constant SNR gains of ST-MRC over ST-SLC [3] and [4] D.S-MRC/T-SLC of about 4.3 and 3.4 dB, respectively, in selective fading for all values of ρ.

From the above SNR results, we compute the corresponding capacity C in terms of number of users per cell with a probability of outage of 1% using the computation procedure in [3]. We assume a speech activity factor equal to 1 with probability $p_{saf} = 0.45$ and 1/8 otherwise [3]. Fig. 4 shows that STAR with the proposed array-receiver enhancements offers a significant increase in capacity over previous solutions [3],[4] in both selective and nonselective fading environments. In nonselective fading, S-MRC provides the best capacity up to a correlation factor around 0.8 while S-MRC/E performs better at higher values of ρ (see semi-dashed curves in Fig. 4a). Their maximum achieves the best capacity over almost the entire correlation range. It offers capacity gains over S-SLC and D.S-MRC/E of about 130 and 90%, respectively, up to a correlation factor around 0.8. These gains degrade dramatically at higher values of ρ. For extreme values of ρ approaching full correlation, S-MRC/E performs nearly as well or worse than D.S-MRC/E. On the other hand, among the 2D-RAKE based structures, S-MRC/T-MRC, S-MRC/T-MRC/E and S-MRC/T-SLC alternatively provide the best

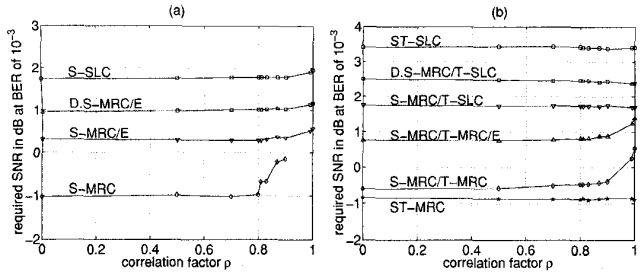

Fig. 3. Required SNR at 9.6 kbps vs. correlation factor ρ for different array-receivers with $M = 2$ antennas. (a): 1.25 MHz system. (b): 5 MHz system.

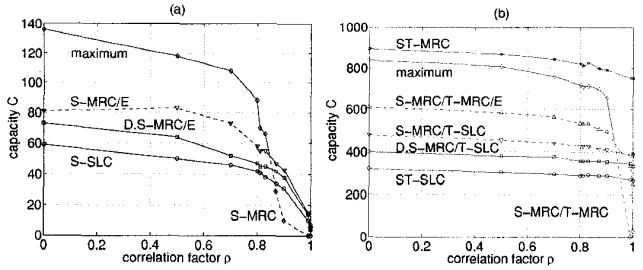

Fig. 4. Capacity C at 9.6 kbps vs. correlation factor ρ for different array-receivers with $M = 2$ antennas. (a): 1.25 MHz system. (b): 5 MHz system.

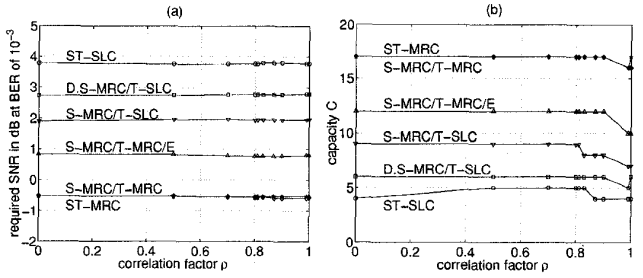

Fig. 5. Performance of the 5 MHz system at 153.6 kbps vs. correlation factor ρ for different array-receivers with $M = 2$ antennas. (a): Required SNR. (b): Capacity C.

capacity in selective fading (see semi-dashed curves in Fig. 4b). The correlation thresholds lie approximately at 0.9 and 0.95. Overall, STAR with ST-MRC offers the highest capacity gains over ST-SLC and D.S-MRC/T-SLC of 180 and 125%, respectively, thereby confirming the advantage of concatenated spatio-temporal combining over 2D-RAKE processing.

Notice that the capacity curves of Fig. 4 partly reflect the behavior of the required SNR curves of Fig. 3, as expected. Other factors such as the received and transmitted power statistics from imperfect power control, not shown for lack of space, also influence the capacity results through incell and outcell interference. In particular, they explain the more severe capacity degradation compared to that of SNR at extreme values of the correlation factor ρ, especially in nonselective fading.

To provide evaluation results for a wideband CDMA application, we simulate data links at 153.6 kbps spread with a processing gain of 32 in the 5 MHz system. We keep the same simulation setup and assume a data activity factor equal to 1 with probability $p_{\text{daf}} = 1$ (*i.e.*, permanent transmission or full capacity). Fig. 5 shows almost constant SNR and capacity curves over the entire range of ρ, suggesting a relatively smaller sensitivity of all array-receivers to correlation at higher data rates, especially with the most sensitive array-receivers. Overall, while the SNR gain of STAR with ST-MRC over previous solutions is almost the same as in Fig. 3, its capacity advantage is more significant.

IV. Conclusions

In this paper we evaluated the performance degradation of different IS-95 CDMA versions of the subspace-tracking array-receiver (STAR) in spatially correlated Rayleigh fading. These versions propose various improvements to better exploit the antenna processing capabilities of a 2D-RAKE structure by coherent detection without a pilot. We also assessed previous array-receiver solutions [3],[4] for comparison. Simulation results confirm that antenna arrays reduce interference significantly even when most of the spatial diversity is lost. The proposed versions that better exploit spatial combining are more sensitive to spatial correlation, especially in nonselective fading or at lower data rates. However, they still offer the best performance even for extreme spatially-correlated conditions. Finally, we exploited the postcorrelation model (PCM) [6] to propose concatenated processing along a single spatio-temporal dimension. This new version of STAR significantly increases robustness to correlation and further improves the performance advantage over 2D-RAKE structures.

References

[1] A.J. Viterbi, *CDMA Principles of Spread Spectrum Communication*, Addison-Wesley, 1995.

[2] *An Overview of the Application of Code Division Multiple Access (CDMA) to Digital Cellular Systems and Personal Cellular Networks*, Qualcomm, Inc., USA, 1992.

[3] A. Jalali and P. Mermelstein, "Effects of diversity, power control, and bandwidth on the capacity of microcellular CDMA systems", *IEEE Journal on Selected Areas in Communications*, vol. 12, no. 5, pp. 952-961, June 1994.

[4] A.F. Naguib and A. Paulraj, "Performance of wireless CDMA with M-ary orthogonal modulation and cell site antenna arrays", *IEEE Journal on Selected Areas in Communications*, vol. 14, no. 9, pp. 1770-1783, December 1996.

[5] S. Affes and P. Mermelstein, "Signal processing improvements for smart antenna signals in IS-95 CDMA", *IEEE PIMRC'98*, Boston, USA, vol. II, pp. 967-972, September 8-11, 1998.

[6] S. Affes and P. Mermelstein, "A new receiver structure for asynchronous CDMA: STAR - the spatio-temporal array-receiver", *IEEE Journal on Selected Areas in Communications*, vol. 16, no. 8, pp. 1411-1422, October 1998.

[7] W.C.-Y. Lee, "Effects on correlation between two mobile radio base-station antennas", *IEEE Transactions on Communications*, vol. 21, no. 11, pp. 1214-1224, November 1973.

[8] F. Adachi, M.T. Feeney, A.G. Williamson, and J.D. Parsons, "Crosscorrelation between the envelopes of 900 MHz signals received at a mobile radio base station site", *IEE Proceedings*, vol. 133, no. 6, pp. 506-512, October 1986.

[9] H. Hansen, S. Affes, and P. Mermelstein, "A beamformer for CDMA with enhanced near-far resistance", *IEEE ICC'99*, Vancouver, Canada, to appear, June 6-10, 1999.

[10] A. Stéphenne and B. Champagne, "A new multi-path vector channel simulator for the performance evaluation of antenna array systems", *IEEE PIMRC'97*, Helsinki, Finland, vol. 3, pp. 1125-1129, September 1-4, 1997.

[11] W.C. Jakes, Ed., *Microwave Mobile Communications*, John Wiley & Sons, 1974.